Atomistic simulation of phonon and alloy limited hole mobility in $Si_{1-x}Ge_x$ nanowires

S. R. Mehrotra*,[1], P. Long[1] M. Povolotskyi[1] and G. Klimeck[1]

[1] Purdue University, West Lafayette - IN , USA

Received XXXX, revised XXXX, accepted XXXX
Published online XXXX

Key words: SiGe,alloy,phonon,mobility

* Corresponding author: e-mail smehrotr@purdue.edu

The role of alloy and phonon scattering is theoretically explored in 5 nm diameter SiGe nanowires at room temperature. Low field mobility calculations are performed by utilizing $sp^3d^5ds^*$-spin-orbit-coupled tight binding model for electronic structure and Boltzmann transport formalism. Three different transport orientations <100>, <110> and <111> are considered. Alloy scattering is found to play an important role in these $Si_{1-x}Ge_x$ nanowires, lending to a characteristic 'U' shaped mobility curve as a function of alloy composition. It is concluded that to extract any advantage of higher Ge hole mobility by alloying, $Ge\%>70\%$ is needed. Furthermore, the <111> channel orientation exhibits the highest hole mobility while <100> has the lowest hole mobility for any given alloy composition.

1 Introduction The SiGe alloy has become a material of interest for p-type metal-oxide-semiconductor field effect transistors (MOSFET) due to the high hole mobility in Ge [1]. SiGe based nanowires are now being explored for improved p-type MOSFETs at short channel lengths making it imperative to understand their transport properties [2]. $Si_{1-x}Ge_x$ is expected to suffer from added alloy disorder besides the scattering due to phonons at room temperature. The role of alloy and phonon scattering in bulk and thin body $Si_{1-x}Ge_x$ structures has been discussed extensively in literature, however, little theoretical work has been done in regard to nanowires [3–5]. In this work the phonon and alloy mobility calculations are performed for 5 nm diameter SiGe nanowires. Different transport orientations i.e. <100>, <110> and <111> are considered as shown in Fig. 1.

2 Simulation Approach The low-field mobility values are calculated based on the linearized Boltzmann transport approach utilizing the $sp^3d^5s^*$ (including spin orbit coupling) tight-binding (TB) model model for the electronic structure [6,7]. The TB parameters for the different compositions of $Si_{1-x}Ge_x$ are calculated based on the previously proposed virtual crystal approximation (VCA) model [8]. The lattice constants (a_0) for the different $Si_{1-x}Ge_x$ compositions are interpolated linearly and the effect of atomic relaxation is neglected. As a first step, band-structure calculations are done for 5 nm diameter $Si_{1-x}Ge_x$ nanowires for three different orientations. Once the electronic structure is computed, momentum re-

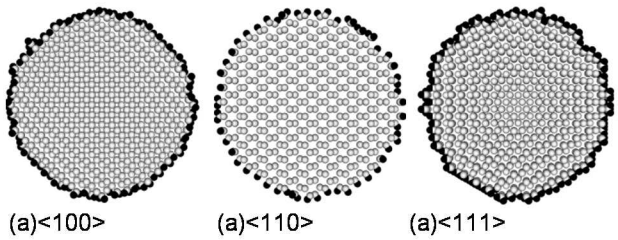

Figure 1 Atomistic representation of H-passivated 5 nm diamater $Si_{1-x}Ge_x$ nanowires for (a) <100> (b) <110> and (c) <111> transport orientations.

laxation rates, $\tau(E)$ and consequently the total mobility, μ is calculated based on the linearized Boltzmann transport model. The general expression for mobility in 1-D nanowires can be written as in Eq. 1 [6].

$$\mu = \frac{q^2 \int \sum_n v_{+k}(E)^2 \tau_{+k}(E) DOS_{+k}(E)(\frac{-df}{dE})dE}{q \int DOS(E) f(E) dE} \quad (1)$$

$v(E)$ is the carrier velocity, $\tau(E)$ is the final integrated momentun relaxation rate and $DOS(E)$ is the total density of states in the units of per unit volume. The $+k$ subscript means that the quantities are calculated only for states moving along $+k$ direction. Scattering rates are calculated for each (per spin) band, n at each energy value, f is the Fermi-Dirac function and q is the charge of an electron. Eq. 1 can be rewritten as:

$$\mu = \frac{q^2 \int \Xi(E)(\frac{-df}{dE})dE}{q \int DOS(E) f(E) dE} \quad (2)$$

where $\Xi(E)$ is the transport distribution (TD) function [6, 10]. TD is directly related to the final mobility term and provides an easy understanding of the interplay between the carrier velocity, density of states and the scattering rates. All the simulations are performed using the NEMO5 simulation package [11].

2.1 Phonon scattering Momentum relaxation rate due to phonons are calculated based on the deformation potential approach. Contributions from both, acoustic and optical phonon modes are considered based on the bulk phonon model [6]. Transition rate for a state in band i to band f due to acoustic (Eq. 3) and optical (Eq. 4) phonon scattering are calculated using the following expression [6]:

$$\frac{1}{\tau^{if}_{ac}(E_i)} = \frac{2\pi}{\hbar} \frac{D^2_{AC} k_B T}{\rho u_l^2} \left(1 - \frac{v_f(k')}{v_i(k)}\right) \frac{I^2_{if}}{L_0} \times \delta[E_f(k') - E_i(k)] \delta_{k', k \pm q_x} \quad (3)$$

$$\frac{1}{\tau^{if}_{op}(E_i)} = \frac{\pi D^2_{OP}}{\rho \omega_0} \left(N_0 + \frac{1}{2} \pm \frac{1}{2}\right) \left(1 - \frac{v_f(k')}{v_i(k)}\right) \frac{I^2_{if}}{L_0} \times \delta[E_f(k') - E_i(k) \pm \hbar\omega_0] \delta_{k', k \pm q_x} \quad (4)$$

where, ρ is the mass density, k_B is the Boltzmann constant , T is the temperature, L_0 is the unit cell length along the transport direction, v is the carrier velocity, u_l is the longitudinal sound velocity, D_{AC} is the effective deformation potential of the acoustic phonon, D_{OP} is the deformation potential of the optical phonon, ω_0 is the frequency of the optical phonon, N_0 is the number of phonons with energy $\hbar\omega_0$ given by the Bose-Einstein distribution, q_x is the momentum of the phonon and δ is the Dirac delta function. Analytical expressions are used for the waveform overlaps given by I^2_{if}. I^2_{if}=$9/4A$ for intra-band and I^2_{if}=$1/A$ for inter-band transistions where A is the cross-section area. All the material parameters for Si and Ge unless mentioned are obtained from Ref. [3] and have been interpolated linearly. The deformation potential values used for Si are, $D_{AC} = 5eV$ and $D_{OP} = 13.24 \times 10^{10} eV/m$ while the deformation potential values used for Ge are, $D_{AC} = 6.65eV$ and $D_{OP} = 8.52 \times 10^{10} eV/m$ [12,13]. The deformation potentials used here have been used to fit experimental data in nanostructures making them more relevant for our case. It should also be noted the values used here are higher than the commonly used bulk values that naturally take into account the changes in phonon bandstructure due to quantum confinement [14].

The use of dispersionless, bulk phonon model provides a simple yet powerful approach towards understanding the effects of bandstructure on mobility in nanoscale devices. Phonon mobility is calculated using the scattering parameters and the approach taken in this work for <100>, <110> and <111> oriented 3 nm diameter Si nanowires. The mobility values are compared against Ref. [9] where phonon limited mobility was calculated using atomistic non-equilibrium quantum transport simulations taking into account the full phonon spectra as shown in Fig. 2. The qualitative trend is well captured using our simple approach. A close quantitative agreement is found for <100>. The deviation increases as the orientation is changed to <110> and <111> as shown in the inset of Fig. 2. Obviously, by adjusting the deformation potential values a good quantitative agreement can still be achieved but it is not the aim of this work. Instead, the same set of deformation potentials for each composition of $Si_{1-x}Ge_x$

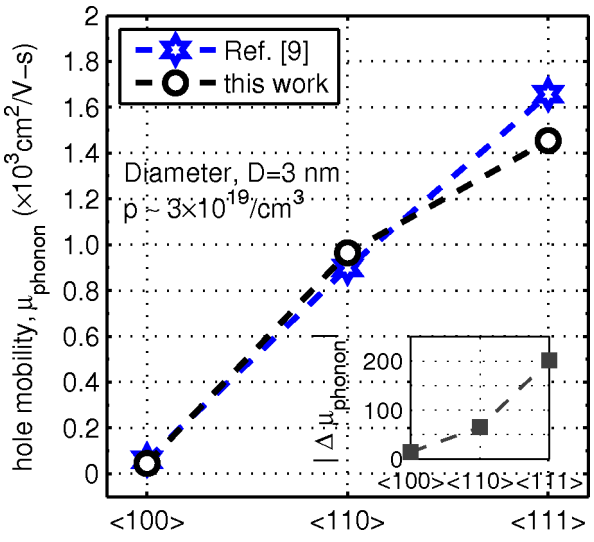

Figure 2 Orientation dependent phonon limited mobility for 3 nm diameter Si nanowire calculated using the approach used in this work and from Ref. [9]. Inset shows the absolute difference in mobility values for different orientations between our model and Ref. [9].

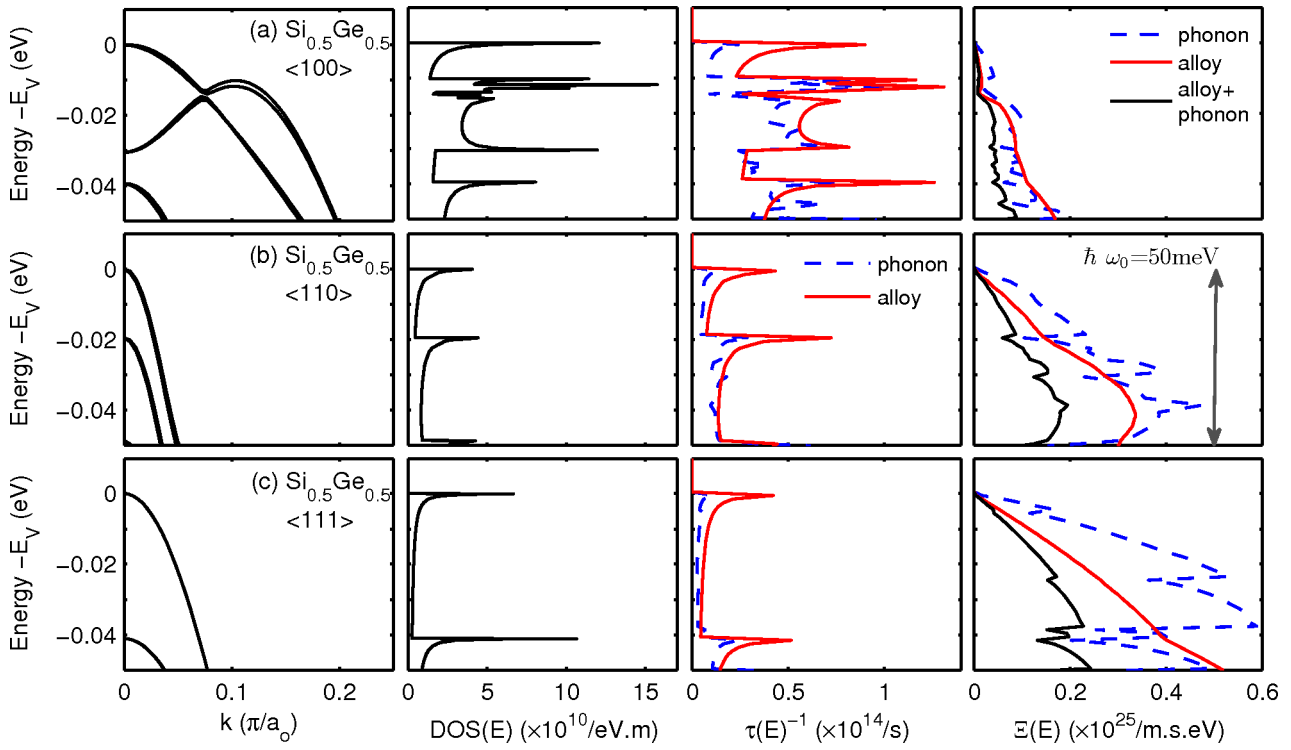

Figure 3 Calculated E-k , DOS(E), $\tau(E)$ and $\Xi(E)$ for (a) <100> (b) <110> and <111> transport oriented 5 nm diameter $Si_{0.5}Ge_{0.5}$ nanowires. The interpolated optical phonon energy for $Si_{0.5}Ge_{0.5}$ $\hbar\omega_0 = 50meV$ is also shown.

have been used for mobility calculations of all the different orientations, as is commonly practiced in literature [6].

2.2 Alloy scattering Alloy scattering is an elastic scattering mechanism that happens when a moving carrier faces a varying potential landscape due different atomic species. An effective scattering potential ΔU is used to describe the strength of the alloy scattering rate [4]. The momentum relaxation rate due to alloy disorder in $Si_{1-x}Ge_x$ can be written as in Eq. 5.

$$\frac{1}{\tau_{al}^{if}(E_i)} = \frac{2\pi}{\hbar}x(1-x)\Delta U^2\Omega\left(1-\frac{v_f(k')}{v_i(k)}\right)\frac{I_{if}^2}{L_0} \times \delta[E_f(k')-E_i(k)]\delta_{|k'|,|k|} \quad (5)$$

Here x is the alloy composition, Ω is the atomic volume which is taken to be $a_0^3/8$ where a_0 is the $Si_{1-x}Ge_x$ lattice constant. The scattering potentials, ΔU used in this work are taken from [4], where the ΔU values were theoretically extracted and the calculated mobility showed a good agreement with the bulk experimental mobility data.

3 Mobility Calculations Fig. 3 shows the E-k relation along with the transport distribution function for $Si_{0.5}Ge_{0.5}$ composition. It can be readily seen that <110> and <111> exhibit lighter bands resulting in reduced density of states compared to the <100> orientation. Since $Si_{0.5}Ge_{0.5}$ will have maximum randomness, alloy scattering is expected to be severe for this composition. The alloy and phonon scattering rates are comparable in strength for the three different orientations. The final TD values ($\Xi(E)$) degrade strongly as the contribution of alloy and phonon scattering mechanism are taken together. The <111> orientation shows higher TD values as compared to <110>, which shows higher TD values compared to <100>. This is a consequence of light bands or low density of states in <111> and <110> which lead to reduced scattering rates and higher TD.

Finally, the total scattering rates, TD and consequently mobility values are calculated for different $Si_{1-x}Ge_x$ compositions and for the different transport orientations. Fig. 4 shows the alloy limited, phonon limited and the total mobility values for the different composition and transport orientations at a low carrier concentration of p=5 $\times$ $10^{18}cm^{-3}$. It can be seen from Fig. 4 that for all the $Si_{1-x}Ge_x$ compositions the total mobility is limited due to phonon scattering. The alloy scattering, however, still plays a significant role by pushing the total mobility down as the $Ge\%$ increases from pure Si before improving back to the pure Si mobility value at a higher $Ge\%$. This leads to the characteristic $'U'$ shaped hole mobility curve similar to previous studies [3]. The $Ge\%$ at which $Si_{1-x}Ge_x$ has its total mobility equal to that of Si is marked in the Fig. 4. It can be seen that to improve upon

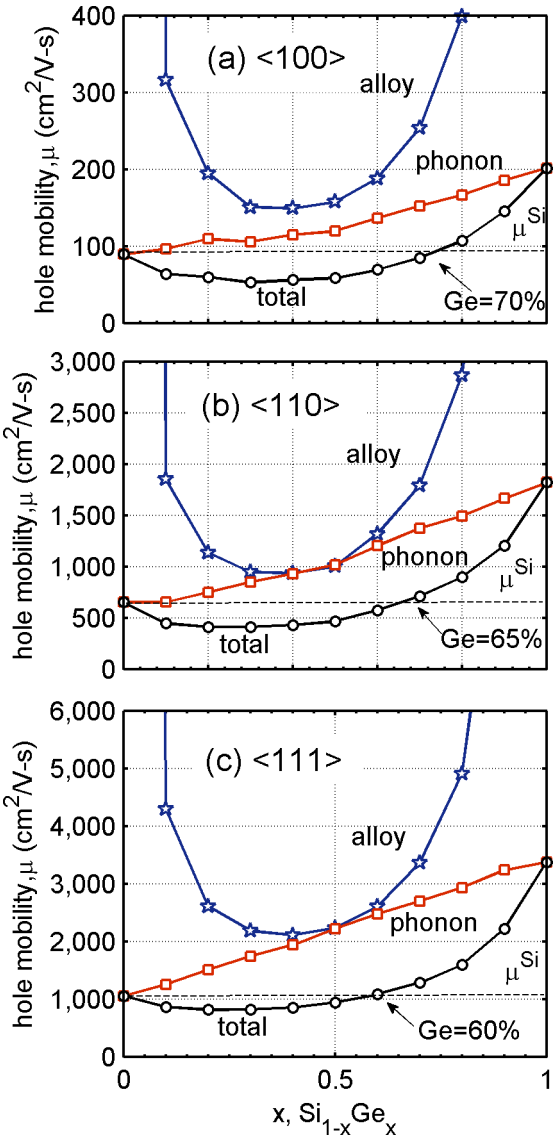

Figure 4 Calculated alloy, phonon and total hole mobility for 5 nm diameter (a) <100> (b) <110> and <111> orientated $Si_{1-x}Ge_x$ nanowires at p=5 $\times$ $10^{18}cm^{-3}$. The $Ge\%$ at which the $Si_{1-x}Ge_x$ mobility matches to that of Si is also marked.

Si atleast $Ge\% > 70\%$ will be needed. Also it found that for any given composition <111> has the highest while <100> has the lowest hole mobilility. Interestingly, taking as an example the case of <100> oriented $Si_{0.5}Ge_{0.5}$ nanowire, ∼8X improvement can be achieved by changing the orientation to <110> or ∼15X improvement by changing the orientation to <111>. These improvements are huge when compared to only ∼3.5X performance enhancement that can be achieved by moving from <100> oriented $Si_{0.5}Ge_{0.5}$ to <100> oriented Ge nanowire, indicating the strong influence of transport orientation in these nanowires.

3.1 Conclusion In this work the role of alloy and phonon scattering on the total mobility is studied in 5 nm diameter $Si_{1-x}Ge_x$ nanowires. Three different transport orientations are considered : <100> , <110> and <111>. Alloy scattering is found to influence the total mobility as the composition is varied in $Si_{1-x}Ge_x$. It is found that atleast $Ge\% > 70\%$ needed to improve upon Si in for any of the transport orientation. Further, it is found that for a given composition of $Si_{1-x}Ge_x$, <111> transport orientation has the highest while <100> has the lowest mobility value.

Acknowledgements The authors would like to thank Materials, Structures and Devices Focus Center, which is one of the six research centers funded under the Focus Center Research Program (a Semiconductor Research Corporation entity) . The use of nanoHUB.org computational resources operated by the Network for Computational Nanotechnology funded by the US National Science Foundation under grant EEC-0228390 is gratefully acknowledged.

References

[1] L. Gomez, C. Ni Chleirigh, P. Hashemi, and J. Hoyt, Electron Device Letters, IEEE **31**(8), 782–784 (2010).
[2] J. Woo Lee, D. Jang, M. Mouis, K. Tachi, G. Tae Kim, T. Ernst, and G. Ghibaudo, Applied Physics Letters **101**(14), 143502–143502 (2012).
[3] M. V. Fischetti and S. E. Laux, Journal of Applied Physics **80**(4), 2234–2252 (1996).
[4] S. R. Mehrotra, A. Paul, and G. Klimeck, Applied Physics Letters **98**(17), 173503 (2011).
[5] A. T. Pham, C. Jungemann, and B. Meinerzhagen, Electron Devices, IEEE Transactions on **54**(9), 2174–2182 (2007).
[6] N. Neophytou and H. Kosina, Physical Review B **84**(8), 085313 (2011).
[7] T. B. Boykin, G. Klimeck, and F. Oyafuso, Physical Review B **69**(11), 115201 (2004).
[8] A. Paul, S. Mehrotra, M. Luisier, and G. Klimeck, Electron Device Letters, IEEE **31**(4), 278 –280 (2010).
[9] M. Luisier, Applied Physics Letters **98**(3), 032111 (2011).
[10] T. J. Scheidemantel, C. Ambrosch-Draxl, T. Thonhauser, J. V. Badding, and J. O. Sofo, Phys. Rev. B **68**(Sep), 125210 (2003).
[11] S. Steiger, M. Povolotskyi, H. H. Park, T. Kubis, and G. Klimeck, Nanotechnology, IEEE Transactions on **10**(6), 1464–1474 (2011).
[12] T. Tanaka, Y. Hoshi, K. Sawano, N. Usami, Y. Shiraki, and K. M. Itoh, Applied Physics Letters **100**(22), 222102 (2012).
[13] A. K. Buin, A. Verma, A. Svizhenko, and M. P. Anantram, Nano Letters **8**(2), 760–765 (2008), PMID: 18205425.
[14] M. Lundstrom, Fundamentals of carrier transport (Cambridge University Press, 2009).